ADVANCES IN LAND SURFACE HYDROLOGY REPRESENTATION IN INM RAS EARTH SYSTEM MODEL

Victor Stepanenko[1]

[1]Lomonosov Moscow State University, Research Computing Center

Contributors:
V.Yu.Bogomolov, V.N.Lykossov, E.M.Volodin, I.Mammarella, H.Miettinen, A.Ojala, T.Vesala, S.P.Guseva, A.Medvedev

International Young Scientists School and Conference, Zvenigorod, 5 September 2017

Пример: снегопады над Великими Американскими озерами (lake-effect snow)

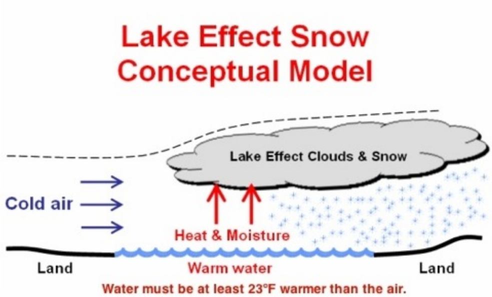

"Озерные снегопады" парализуют дорожную ситуацию, закрываются школы, отменяются полеты и т.д. В течение XX в. наблюдается тренд увеличение суммы снежных осадков в данном районе, $+1.9$ см год$^{-1}$.

При холодных вторжениях континентального воздуха интенсивное испарение и конвекция приводят к образованию облачности и осадков.

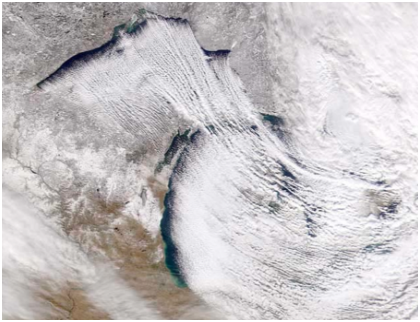

Example: convection over Great African Lakes

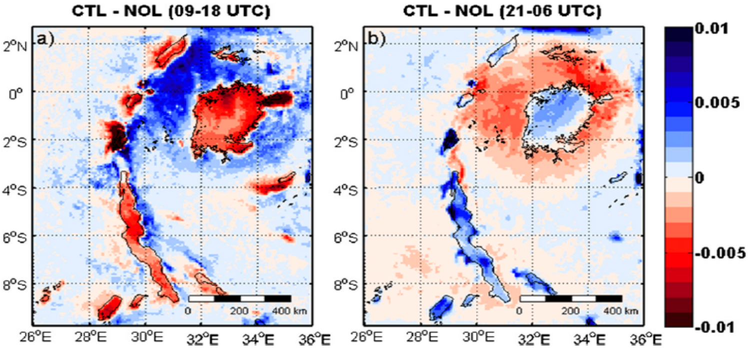

FIG. 15. The 1999–2008 mean change in convective mass flux density at cloud-base height (kg m^{-2} s^{-1}) induced by lake presence, for (a) 0900–1800 UTC (daytime) and (b) 2100–0600 UTC (nighttime).

Nocturnal convection over Victoria accounts for annual fishers death toll $\sim$ 5000.

Thiery et al. 2015, J. of Climate, DOI: 10.1175/JCLI-D-14-00565.1

Example: cloudiness over the Ladoga Lake

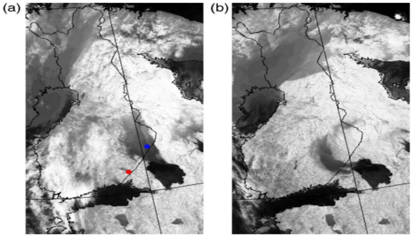

Fig. 3. NOAA AVHRR thermal IR images over Finland and Karelia on 28 January 06 UTC (a) and on 29 January 00 UTC (b) 2012. The low-level cloud cover, shown with dark-grey shades, spreads first northward (a) and later westward (b) from Lake Ladoga. In the single-channel images, the cloud over Lake Ladoga cannot be distinguished from the dark water surfaces. The stations

Ice-free lake evaporates, and resulting stratiform clouds are advected to Finland.

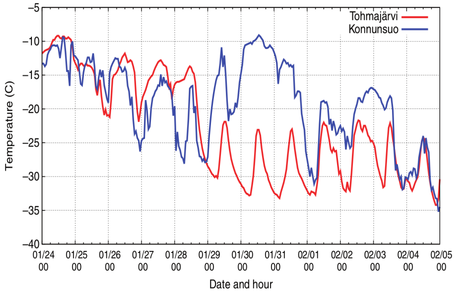

Cloudiness increases the surface net radiation, and 2m-temperature rises by 15-20$°C$

Eerola et al. Tellus A 2014, 66, 23929, http://dx.doi.org/10.3402/tellusa.v66.23929

Freshwaters in global carbon cycle

(Tranvik et al. 2009)

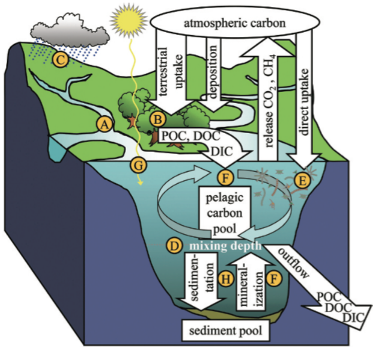

Fig. 2. Schematic diagram showing pathways of carbon cycling mediated by lakes and other continental waters. The letters correspond to rows in Table 1.

(Bastviken et al. 2011)

Latitude	Fluxes: Total open water Emiss.	n	CV	Ebullition Emiss.	n	CV	Diffusive Emiss.	n	CV	Stored Emiss.	n	CV	Area (km^2)
Lakes													
>66°	6.8	17	72	6.4	17	74	0.7	60	37				288,318
>54°–66°	6.6	5	155	9.1	9	60	1.1	271	185	0.1	217	2649	1,533,084
25°–54°	31.6	15	127	15.8	15	177	4.8	33	277	3.7	36	125	1,330,264
<24°	26.6	29	51	22.2	28	54	3.1	29	97	21.3	1		585,536*
Reservoirs													
>66°	0.2†												35,289
>54°–66°	1.0	24	176	1.8	2	140	0.2	4	93				161,352
25°–54°	0.7‡												116,922
<24°	18.1	11	87										186,437
Rivers													
>66°	0.1	1											38,895
>54°–66°	0.2†												80,009
25°–54°	0.3	20	302										61,867
<24°	0.9‡												176,856
Sum open water	93.1	116		55.3	71		9.9	397		25.1	254		
Plant flux	10.2												
Sum all	103.3												

- Total freshwater methane emission is 104 Tg yr^{-1}, i.e. 50% of global wetland emission (177-284 Tg yr^{-1}, IPCC, 2013)
- greenhouse warming potentials from freshwater-originating CO_2 and CH_4 are roughly equal

CO_2 emissions by lakes and rivers

Raymond et al., 2013, Nature

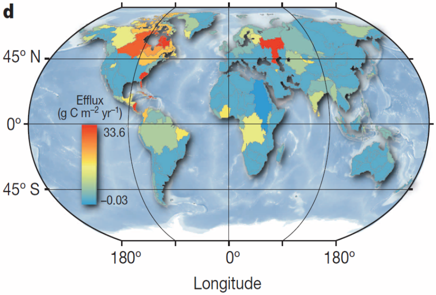

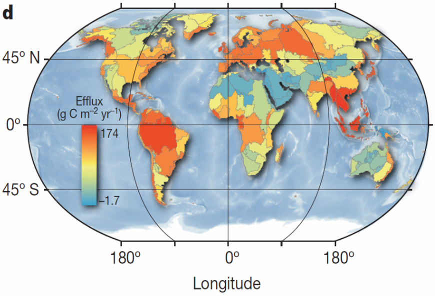

Водоемы

Водотоки

- global emission of CO_2 by freshwaters is 2.1 Pg C yr^{-1}
- lake emission is 0.3 Pg C yr^{-1}, river emissions is 1.8 Pg C yr^{-1}
- significant contribution of Volga hydropower reservoirs

Эмиссия парниковых газов из водохранилищ

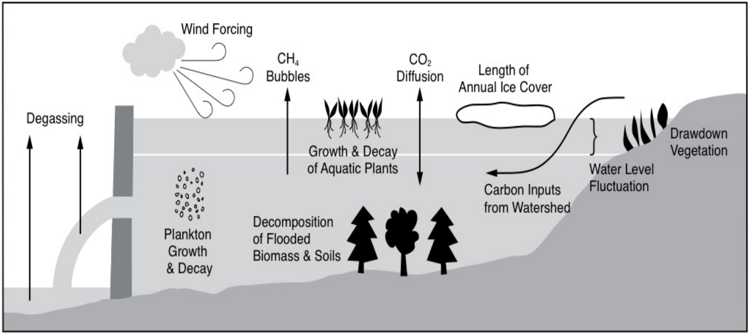

- Затопленные экосистемы подвергаются длительному разложению в преимущественно анаэробных условиях
- В отличие от естественных водоемов, имеется дополнительный путь для эмиссии метана в атмосферу – через турбины

Global warming of lakes

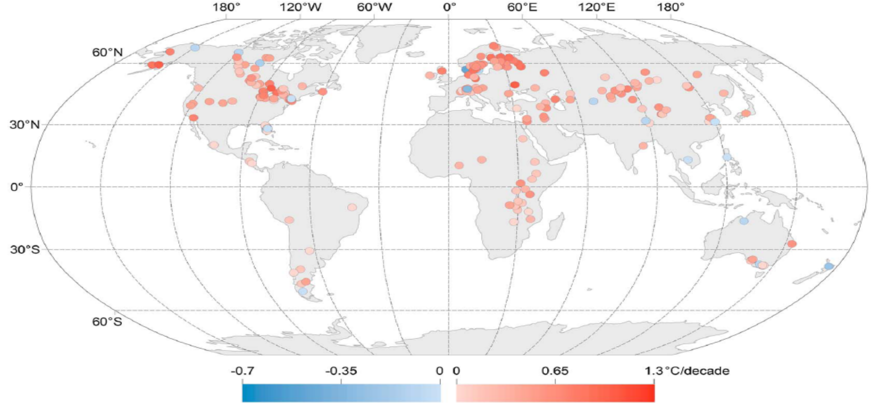

Figure 1. Map of trends in lake summer surface temperatures from 1985 to 2009. Most lakes are warming, and there is large spatial heterogeneity in lake trends. Note that the magnitudes of cooling and warming are not the same.

The majority of lakes are warming at a rate higher than T_{2m}.

O'Reilly et al., 2015, GRL, doi:10.1002/ 2015GL066235

1D lake model framework

1D equations result from boundary-layer approximation

- 1D heat and momentum equations
- $k - \epsilon$ turbulence closure
- Monin-Obukhov similarity for surface fluxes
- Beer-Lambert law for shortwave radiation attenuation
- Momentum flux partitioning between wave development and currents (Stepanenko et al., 2014)
- Soil heat and moisture transfer including phase transitions
- Multilayer snow and ice models

1D concept does not suffice the greenhouse gas modeling task, as it does not take into account differences between CH_4 & CO_2 emissions at deep and shallow sediments

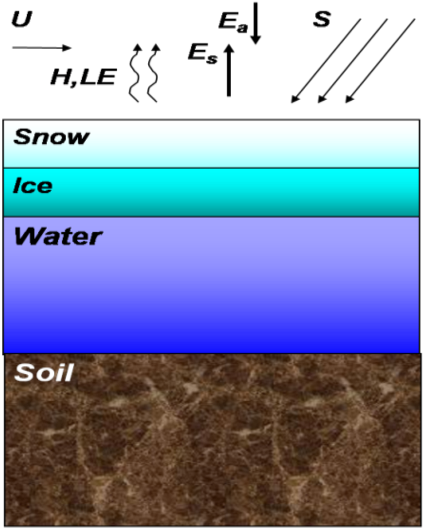

$k-\epsilon$ turbulence closure

$$\overline{w'\phi'} = -k_\phi \frac{\partial \overline{\phi}}{\partial z}$$

- counter-gradient effects missing

Kolmogorov formula (1942)

$$\boxed{k_M = C_e \frac{E^2}{\varepsilon}}, \qquad C_e = C_e(M,N)$$

$$k_T = k_S = C_{eT}\frac{E^2}{\varepsilon}, \qquad C_{eT} = C_{eT}(M,N)$$

M – friction frequency,
N – Brunt-Vaisala frequency

stability functions

k-ε parameterization

$$\frac{\partial E}{\partial t} = \frac{\partial}{\partial z}\left(\nu + \frac{k_M}{\sigma_E}\right)\frac{\partial E}{\partial z} + P + B - \varepsilon$$

$$\frac{\partial \varepsilon}{\partial t} = \frac{\partial}{\partial z}\left(\nu + \frac{k_M}{\sigma_\varepsilon}\right)\frac{\partial \varepsilon}{\partial z} + \frac{\varepsilon}{E}\left(c_{1\varepsilon}P + c_{3\varepsilon}B - c_{2\varepsilon}\varepsilon\right)$$

Boundary conditions

$$-\frac{k_M}{\sigma_E}\frac{\partial E}{\partial z} = c_{we}\left(\frac{\tau_s}{\rho_w}\right)^{3/2}, \quad c_{we} \approx 100$$

$$-\frac{k_M}{\sigma_\varepsilon}\frac{\partial \varepsilon}{\partial z} = \left(C_e^0\right)^{3/4}\frac{k_M}{\sigma_\varepsilon}\frac{E^{3/2}}{\kappa(z'+z_0)^2}$$

$1D^+$ framework

Traditional 1D model concept

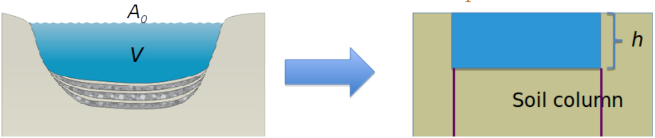

$1D^+$ model concept

- $1D^+$ model includes friction, heat and mass exchange at the lateral boundaries
- Heat, moisture and gas transfer are solved for each soil column independently

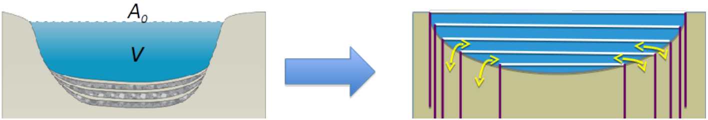

In $1D^+$ model horizontally averaged quantity f obeys the equation:

$$\frac{\partial f}{\partial t} = \frac{1}{A}\frac{\partial}{\partial z} A k_f \frac{\partial f}{\partial z} + F(z,t,f,A) + H_f \frac{1}{A}\frac{dA}{dz}.$$

Coupling heat transport in water and soil

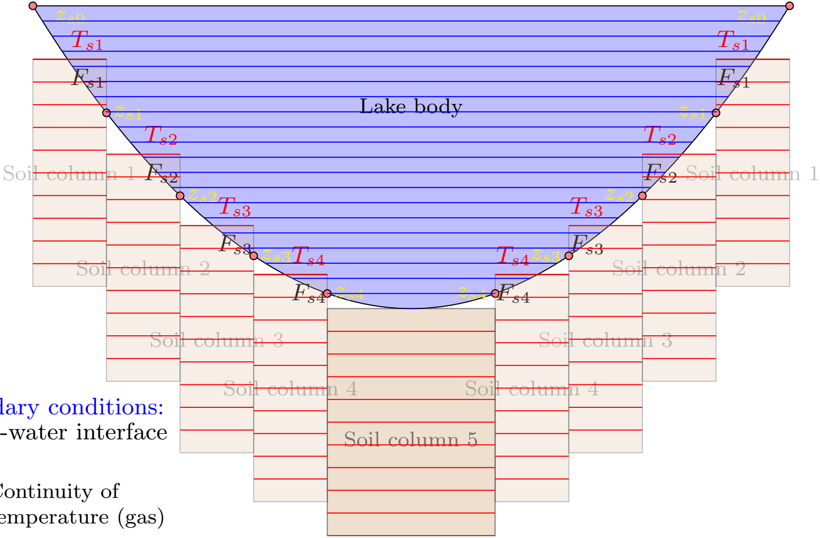

Boundary conditions:
at soil-water interface

- Continuity of temperature (gas)
- Continuity of flux

1D equations for enclosed basins

Horizontally-averaged 3D equations for basic prognostic quantities:

$$c_w \rho_w \frac{\partial \overline{T}}{\partial t} = \cdots \frac{1}{A} \frac{\partial}{\partial z} \left(A \left(\lambda_m + c_w \rho_w \nu_T \right) \frac{\partial \overline{T}}{\partial z} \right) -$$

$$- \frac{1}{A} \frac{\partial A \overline{S}}{\partial z} + \frac{1}{A} \frac{dA}{dz} [S_b + F_{T,b}(z)], \quad \text{– heat conservation equation} \qquad (1)$$

$$\frac{\partial \overline{u}}{\partial t} = \cdots \boxed{- \overline{\left(\frac{1}{\rho_w} \frac{\partial p}{\partial x} \right)}} + \frac{1}{A} \frac{\partial}{\partial z} \left(A(\nu + \nu_m) \frac{\partial \overline{u}}{\partial z} \right) +$$

$$+ \frac{1}{A} \frac{dA}{dz} F_{u,b}(z) + f \overline{v}, \quad \text{– momentum equation for x-speed component} \qquad (2)$$

$$\frac{\partial \overline{v}}{\partial t} = \cdots \boxed{- \overline{\left(\frac{1}{\rho_w} \frac{\partial p}{\partial y} \right)}} + \frac{1}{A} \frac{\partial}{\partial z} \left(A(\nu + \nu_m) \frac{\partial \overline{v}}{\partial z} \right) +$$

$$+ \frac{1}{A} \frac{dA}{dz} F_{v,b}(z) - f \overline{u} \quad \text{– momentum equation for y-speed component} \qquad (3)$$

Barotropic pressure gradient and seiches

Barotropic (surface) seiches are lake surface and related velocity oscillations after strong wind events.

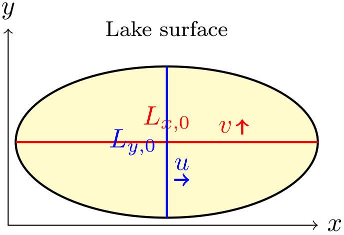

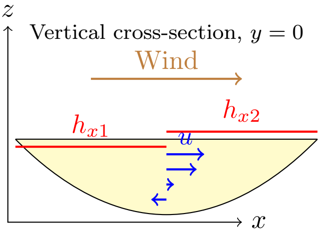

Turbulent kinetic energy profile (modeled), June 2013, Kuivajarvi Lake, seiches produce TKE near bottom

Mass conservation
$$\begin{cases} \frac{dh_N}{dt}A_0(t) = -\frac{dh_S}{dt}A_0(t) = 2\int_0^1 vL_{W-E}hd\xi, \\ \frac{dh_E}{dt}A_0(t) = -\frac{dh_W}{dt}A_0(t) = 2\int_0^1 uL_{S-N}hd\xi, \end{cases}$$

Barotropic pressure gradient force
$$\begin{cases} g\overline{\frac{\partial h_s}{\partial x}} \approx \frac{g\pi^2}{4}\frac{h_E - h_W}{L_{W-E,0}}, \\ g\overline{\frac{\partial h_s}{\partial y}} \approx \frac{g\pi^2}{4}\frac{h_N - h_S}{L_{S-N,0}}. \end{cases}$$

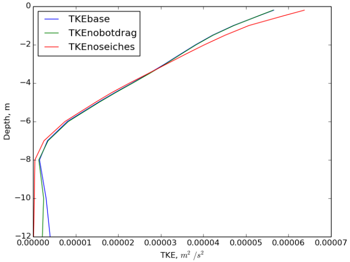

Surface oscillations in the model

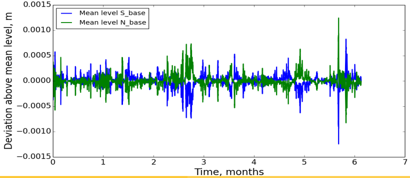

Biogeochemical processes in the model

- Photosynthesis, respiration and BOD are empirical functions of temperature and Chl-a (Stefan and Fang, 1994)
- Oxygen uptake by sediments (SOD) is controlled by O_2 concentration and temperature (Walker and Snodrgass, 1986)
- Methane production $\propto P_0 q_{10}^{T-T_0}$, P_0 is calibrated (Stepanenko et al., 2011)
- Methane oxidation follows Michaelis-Menthen equation

Sinks and sources of gases in a lake

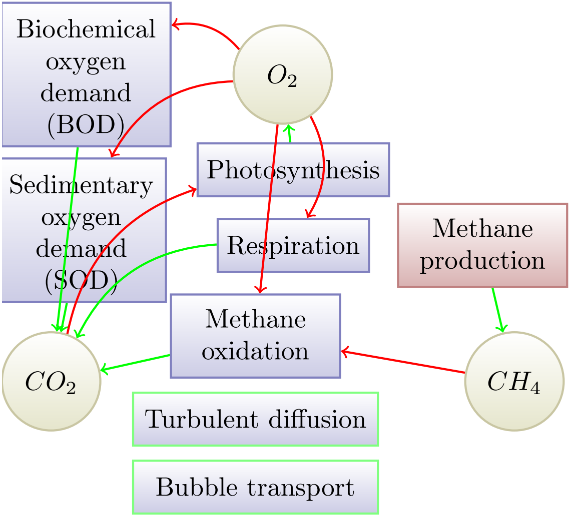

Model validation for Seida Lake

Guseva et al., Geogr. Env. Sust., 2016

Seida lake location

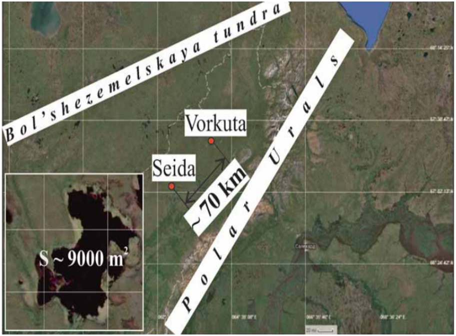

Bubble flux (starting from 01.07.2007)

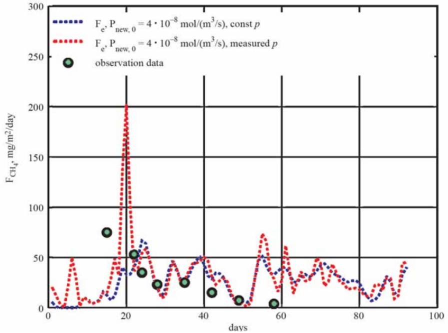

Table 3. Methane production rate constant $P_{new,0}$ in other studies

$P_{new,0}$ (mol · m^{-3} · s^{-1})	Source
$3.0 \cdot 10^{-8}$	Lake Kuivajärvi, Finland [Stepanenko et al., 2016]
$2.55 \cdot 10^{-8}$	Shuchi Lake, North Eastern Siberia, Russia [Stepanenko et al., 2011]
$8.3 \cdot 10^{-8} - 1.6 \cdot 10^{-7}$	High latitude wetlands [Walter & Heimann, 2000]
$4.0 \cdot 10^{-8}$	Lake at the Seida site, current study

Kuivajärvi Lake (Finland)

- Mesotrophic, dimictic lake
- Area 0.62 km^2 (length 2.6 km, modal fetch 410 m)
- Altitude 142 m a.s.l.
- Maximal depth 13.2 m, average depth 6.4 m, deptl the point of measurements 12.5 m
- Catchment area 9.4 km^2

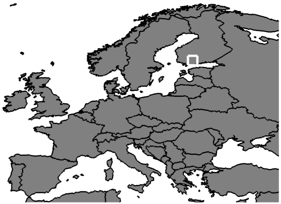

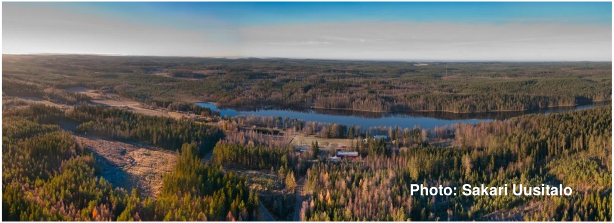

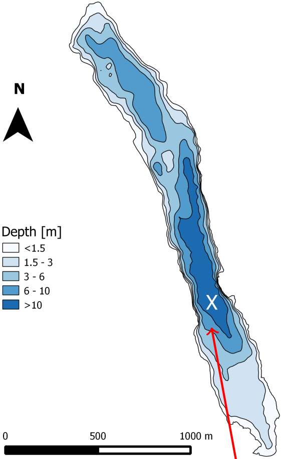

Point of measurements

Measurements

- Conducted since 2009 by University of Helsinki
- Ultrasonic anemometer USA-1, Metek GmbH
- Enclosed-path infrared gas analyzers, LI-7200, LI-COR Inc.
- Four-way net radiometer (CNR-1)
- relative humidity at the height of 1.5 m (MP102H-530300, Rotronic AG)
- thermistor string of 16 Pt100 resistance thermometers (depths 0.2, 0.5, 1.0, 1.5, 2.0, 2.5, 3.0, 3.5, 4.0, 4.5, 5.0, 6.0, 7.0, 8.0, 10.0 and 12.0 m)
- Turbulent fluxes were calculated from 10 Hz raw data by EddyUH software

Measurement raft

Footprint of the raft measurements

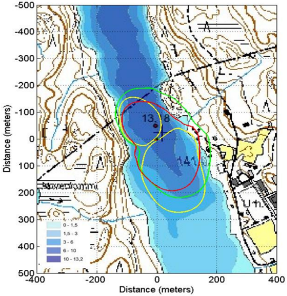

Water temperature

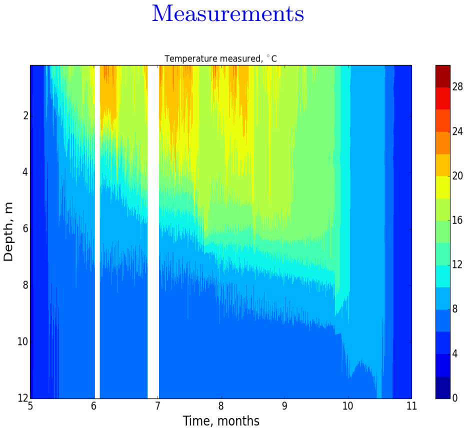

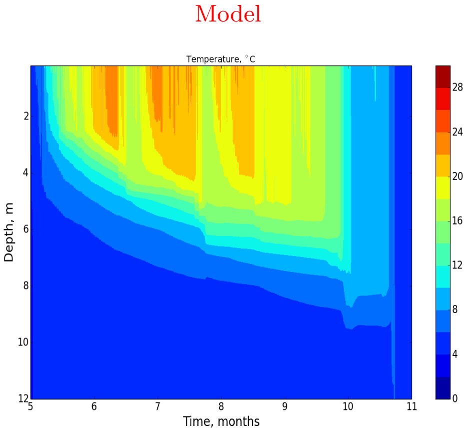

- Mixed layer depth and surface temperature (RMSE=1.54 °C) are well reproduced
- Stratification strength in the thermocline is overestimated
- Model results lack frequent temperature oscillations in the thermocline

Oxygen

Stepanenko et al., Geosci. Mod. Dev., 2016

Measurements

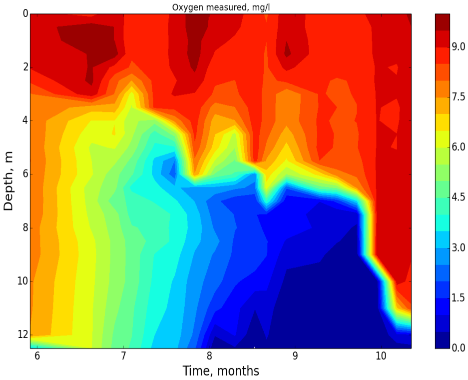

Model

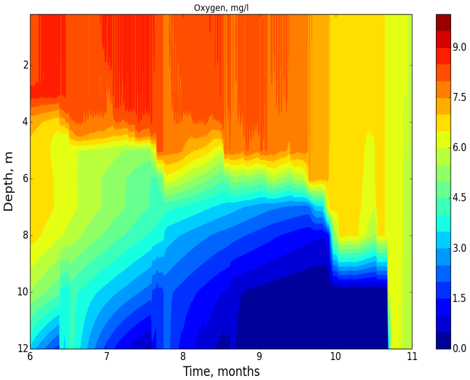

- Seasonal pattern is well captured: oxygen is produced in the mixed layer and consumed below
- Oxygen concentration in the mixed layer is underestimated by 1-1.5 mg/l, and more significantly during autumn overturn

Carbon dioxide concentration

Stepanenko et al., Geosci. Mod. Dev., 2016

Measurements

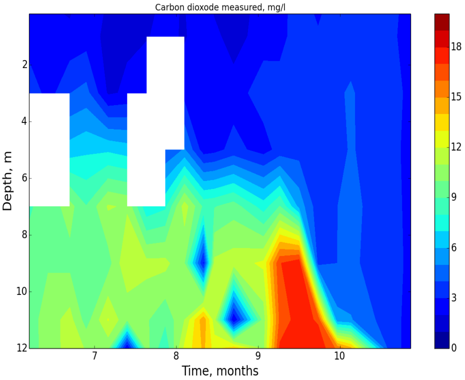

Model

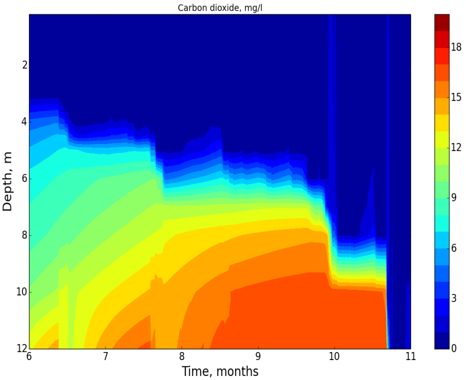

- Seasonal pattern is simulated realistically: carbon dioxide is consumed by photosynthesis in the mixed layer and produced in the thermocline and hypolimnion by aerobic organics decomposition
- Sudden CO_2 increase prior to autumn overturn is absent in the model

Methane

Stepanenko et al., Geosci. Mod. Dev., 2016

Measurements

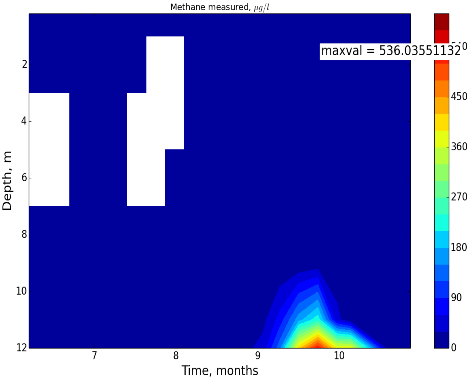

Model

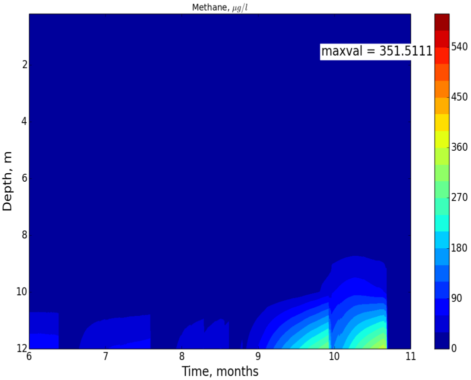

- Methane starts to accumulate near bottom in the late summer when oxygen concentration drops to low values
- Surface methane concentration is very small leading to negligible diffusive flux to the atmosphere, consistent with measurements

Further development: dissolved and particulate carbon

Adopting approach from Hanson et al., 2004

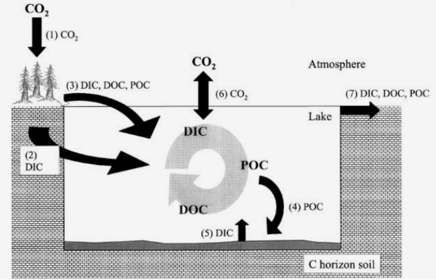

- The Hanson et al. model is reformulated to explicitly reproduce vertical distribution of DOC, POCL, POCD (instead of using mixed-layer and hypolimnion pools, as in original paper)
- The horizontal influx from catchment is to be included

Extended biogeochemical model

$$\frac{\partial C_{CH_4}}{\partial t} = Dif_A(C_{CH_4}) + B_{CH_4} - O_{CH_4}, \quad (1)$$

$$\frac{\partial C_{O_2}}{\partial t} = \mathrm{Dif}_A(C_{O_2}) + B_{O_2} + P_{O_2} - R_{O_2} - D_{O_2} - S_{O_2} - O_{O_2}, \quad (2)$$

$$\frac{\partial C_{DIC}}{\partial t} = \mathrm{Dif}_A(C_{DIC}) + B_{CO_2} - P_{CO_2} + R_{CO_2} + D_{CO_2} + S_{CO_2} + O_{CO_2}, \quad (3)$$

$$\boxed{\frac{\partial \rho_{DOC}}{\partial t} = \mathrm{Dif}(\rho_{DOC}) + E_{POCL} - D_{DOC}}, \quad (4)$$

$$\boxed{\frac{\partial \rho_{POCL}}{\partial t} = \mathrm{Dif}(\rho_{POCL}) + P_{POCL} - R_{POCL} - E_{POCL} - D_{h,POCL}}, \quad (5)$$

$$\boxed{\frac{\partial \rho_{POCD}}{\partial t} = \mathrm{Dif}(\rho_{POCD}) - \frac{w_g}{h}\frac{\partial \rho_{POCD}}{\partial \xi} - D_{POCD} + D_{h,POCL}}. \quad (6)$$

Схема включения модели водоемов Lake в модель INMCM

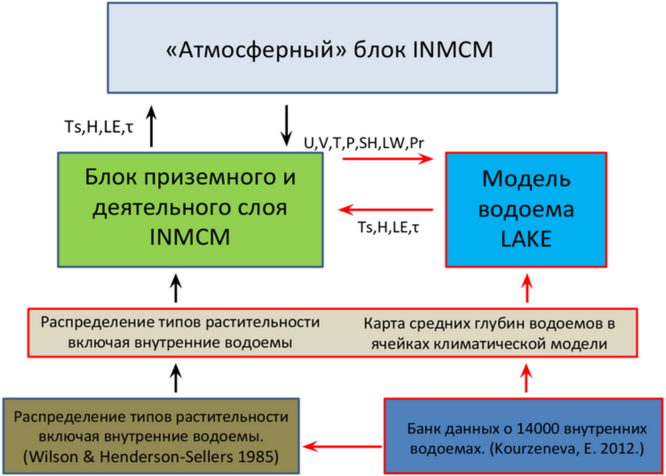

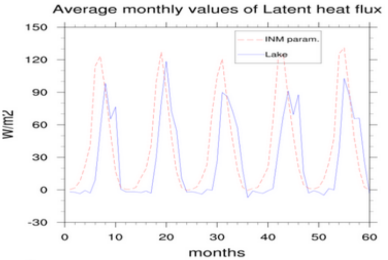

Средне месячные значения потоков скрытого тепла для озера Байкал за 5 лет

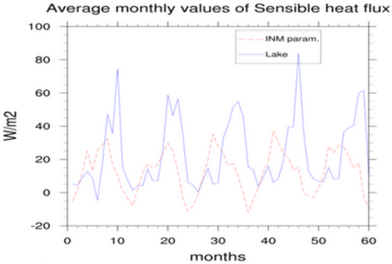

Средне месячные значения потоков явного тепла для озера Байкал за 5 лет

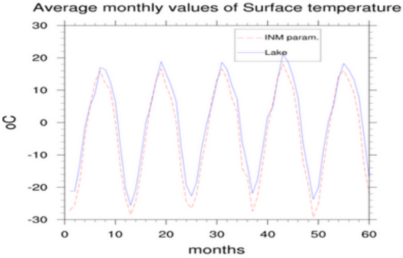

Средне месячные значения температуры поверхности для озера Байкал за 5 лет

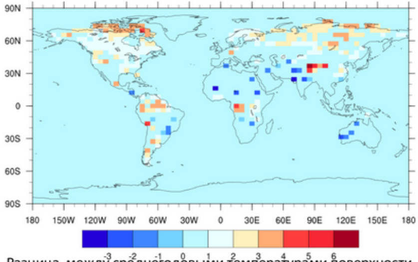

Разница между среднегодовыми температурами поверхности водоемов из модели LAKE и модели INMCM

Motivation for inclusion of rivers in ESMs

- river runoff affects thermohaline circulation
- river runoff is the most precisely measured component of the land water balance
- rivers are considered as an substantial player in land carbon cycle
- the level and ice regimes of rivers can become the one of the most in-demand output of ESMs

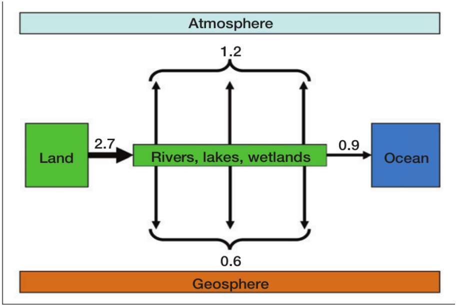

All values are in Pg C yr^{-1} (Battin et al., 2009)

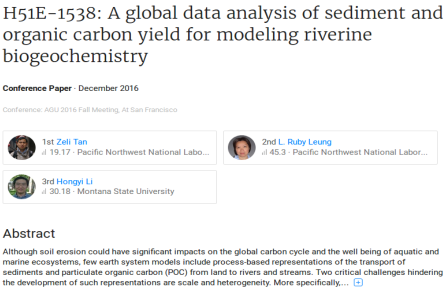

H51E-1538: A global data analysis of sediment and organic carbon yield for modeling riverine biogeochemistry

Conference Paper · December 2016

Conference: AGU 2016 Fall Meeting, At San Francisco

1st Zeli Tan
19.17 · Pacific Northwest National Labo...

2nd L. Ruby Leung
45.3 · Pacific Northwest National Labor...

3rd Hongyi Li
30.18 · Montana State University

Abstract

Although soil erosion could have significant impacts on the global carbon cycle and the well being of aquatic and marine ecosystems, few earth system models include process-based representations of the transport of sediments and particulate organic carbon (POC) from land to rivers and streams. Two critical challenges hindering the development of such representations are scale and heterogeneity. More specifically,...

River runoff in INMCM model

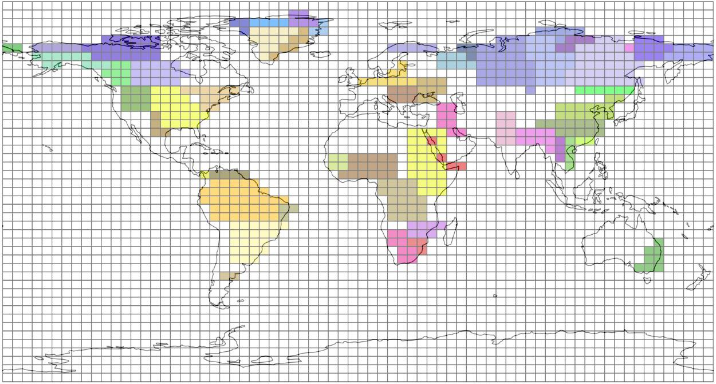

- 54 major basins
- surface and subsurface runoff are integrated over basins and instantaneously "added" to oceans in salinity equation
- no river tile in the surface energy balance calculations

River routing for Earth System Models

Exemplified by (Yamazaki et al., 2009)

Stream upscaling

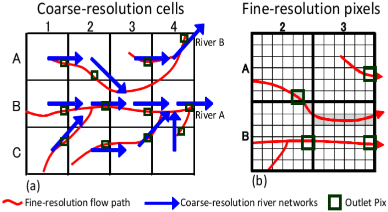

External parameters for river model:

- flow direction
- riverbed slope
- parameters of cross-section geometry

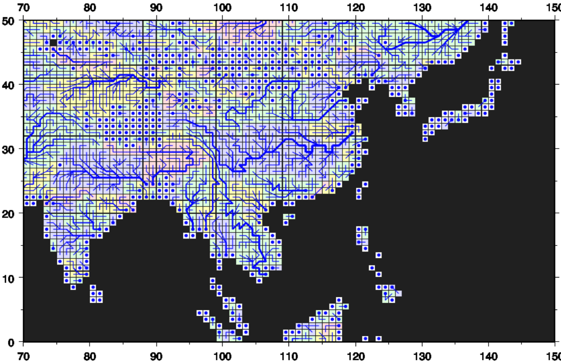

Fig. 6. Illustration of the Monsoon Asian part of an upscaled river network map at the resolution of 1 degree. Bold blue lines indicate riv channels of the upscaled river network map, and circles indicate cells representing a river mouth.

Riverflow dynamic equations

Saint-Venant system:

$$\frac{\partial S}{\partial t} + \frac{\partial SU}{\partial x} = E_r,$$

$$\boxed{\frac{\partial SU}{\partial t} + \frac{\partial SU^2}{\partial x}} = -g\frac{\partial (h_b + h_r)}{\partial x} - \frac{gU^2}{C^2(R)R} + \frac{\partial}{\partial x}\nu_r\frac{\partial U}{\partial x},$$

$$h_r = f(S).$$

- Highlighted are inertia terms that can be omitted if $\mathrm{Fr} \doteq \frac{U^2}{g(\Delta h_b + \Delta h_r)} \ll 1$
- $|\frac{\partial h_r}{\partial x}| \ll |\frac{\partial h_b}{\partial x}|$ at $\mathrm{Fr} < 0.1$ (Dingman, 1984)
- Longitudinal viscosity effects are also considered small

Using $\Delta h_b = \frac{\partial h_b}{\partial x}\Delta x = s\Delta x$, Froude number criterium becomes

$$\Delta x > \frac{10U^2}{gs} \sim 100 \text{ m for plain rivers.}$$

Under these conditions comes Manning's equation:

$$\boxed{U = \frac{1}{n}R^{2/3}s^{1/2}}.$$

Outlook

-> introducing of POC and DOC dynamics in lakes to improve CO_2 simulations

-> introducing nutrient dynamics in lakes

-> simulations of future climate with lakes embedded in INMCM ESM (with both thermodynamic and biogeochemical coupling)

-> testing river dynamics module in INMCM land surface scheme

The work is supported by grants RSF 17-17-01210 and RFBR 17-05-01165

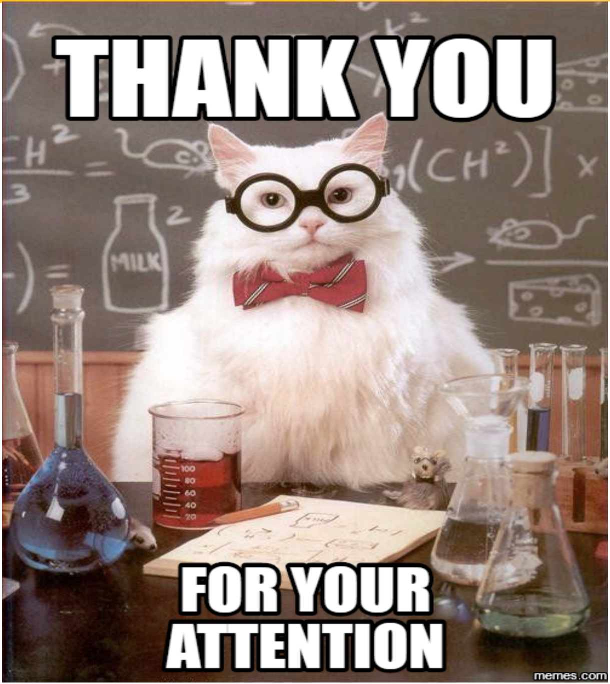
THANK YOU
MILK
FOR YOUR ATTENTION
memes.com

Soil columns in the model

Horizontal projection

Soil columns are geometric figures of the same vertical dimension and with horizontal sections confined by sequential isobaths:

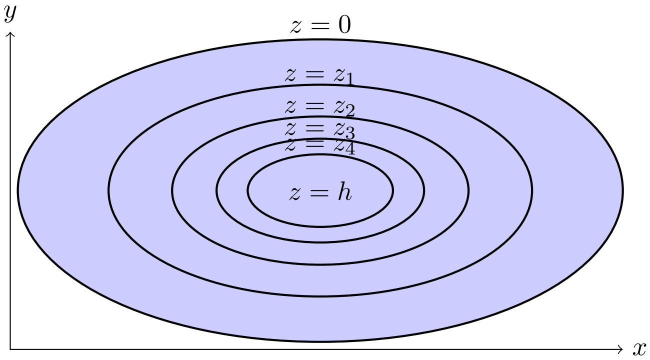

Freshwaters in global carbon cycle

(Tranvik et al. 2009)

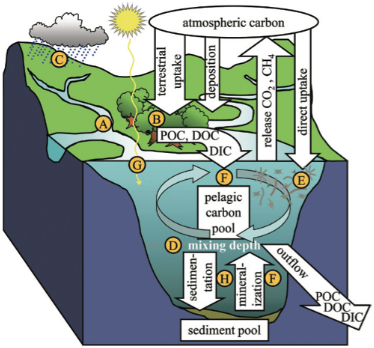

Fig. 2. Schematic diagram showing pathways of carbon cycling mediated by lakes and other continental waters. The letters correspond to rows in Table 1.

(Bastviken et al. 2011)

Latitude	Fluxes: Total open water Emiss.	*n*	CV	Ebullition Emiss.	*n*	CV	Diffusive Emiss.	*n*	CV	Stored Emiss.	*n*	CV	Area (km^2)
Lakes													
>66°	6.8	17	72	6.4	17	74	0.7	60	37				288,318
>54°–66°	6.6	5	155	9.1	9	60	1.1	271	185	0.1	217	2649	1,533,084
25°–54°	31.6	15	127	15.8	15	177	4.8	33	277	3.7	36	125	1,330,264
<24°	26.6	29	51	22.2	28	54	3.1	29	97	21.3	1		585,536*
Reservoirs													
>66°	0.2†												35,289
>54°–66°	1.0	24	176	1.8	2	140	0.2	4	93				161,352
25°–54°	0.7‡												116,922
<24°	18.1	11	87										186,437
Rivers													
>66°	0.1	1											38,895
>54°–66°	0.2†												80,009
25°–54°	0.3	20	302										61,867
<24°	0.9‡												176,856
Sum open water	93.1	116		55.3	71		9.9	397		25.1	254		
Plant flux	10.2												
Sum all	103.3												

- Total freshwater methane emission is 104 Tg yr^{-1}, i.e. 50% of global wetland emission (177-284 Tg yr^{-1}, IPCC, 2013)
- greenhouse warming potentials from freshwater-originating CO_2 and CH_4 are roughly equal

Thermocline thickness

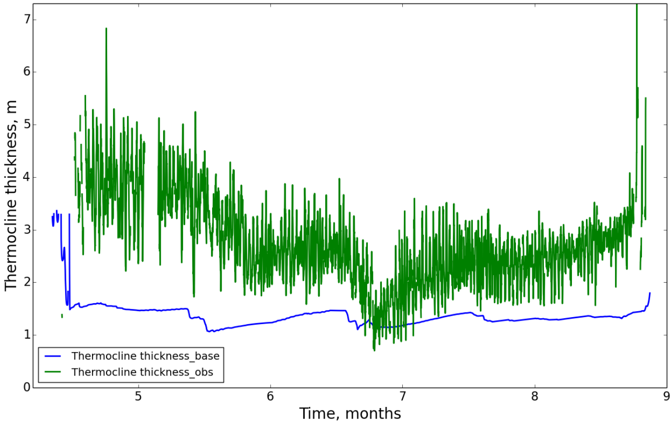

Thermocline thickness is defined as a depth difference between 8 °C and 14 °C isotherms

Methane budget in the surface mixed layer

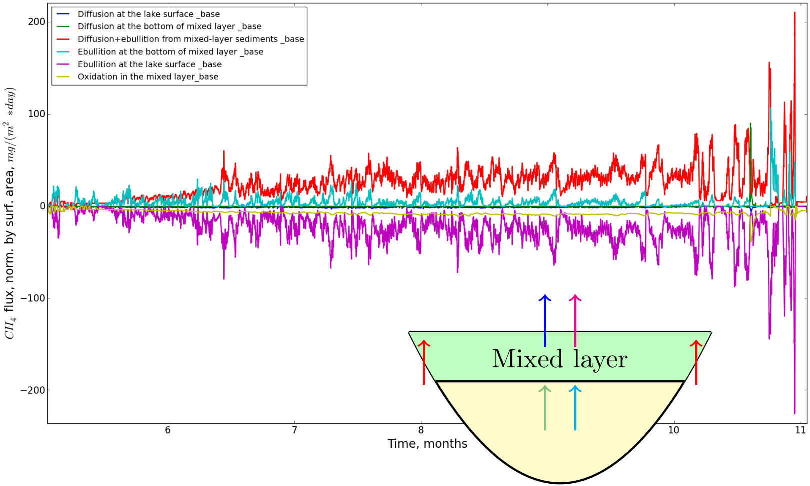

The diffusive flux through thermocline is negligible compared to other terms

TKE profiles

TKE

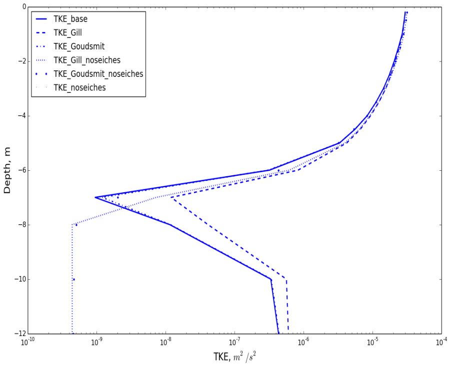

TKE balance terms

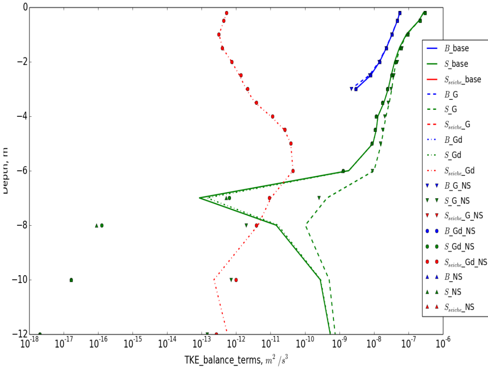

Significance of Coriolis force for Kuivajärvi Lake

Rossby deformation number, $\mathrm{Ro} = \frac{NH}{f} \approx \frac{\sqrt{g\rho_0^{-1}\Delta\rho\ h_{ML}}}{f}$

The lake's length

Rotational effects are comparable with those of stratification.

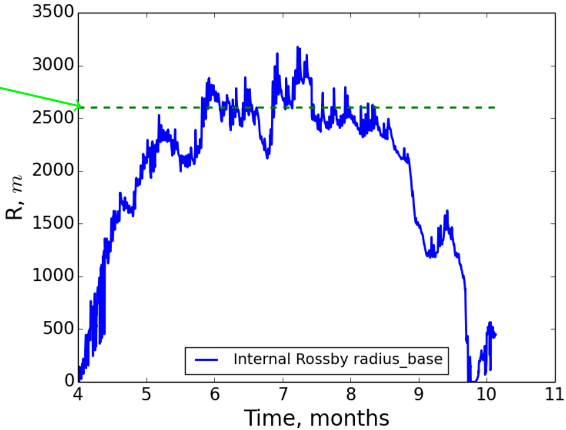

The effect of barotropic seiches on methane

Control simulation

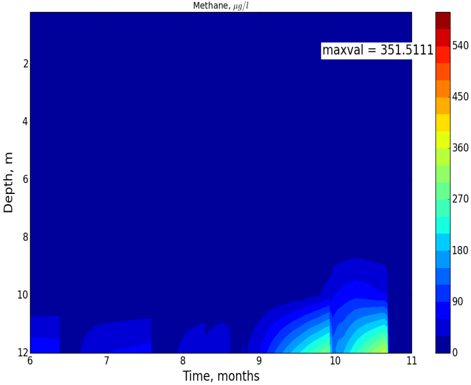

Seiches excluded

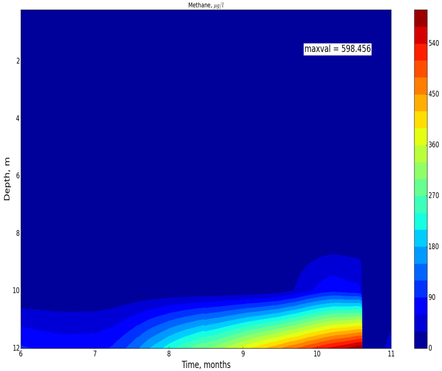

Neglecting barotropic seiches leads to $TKE \approx 0$ below thermocline, less oxygen flux from above and earlier accumulation of methane near bottom

Effect of weak turbulent mixing in the thermocline

Control simulation

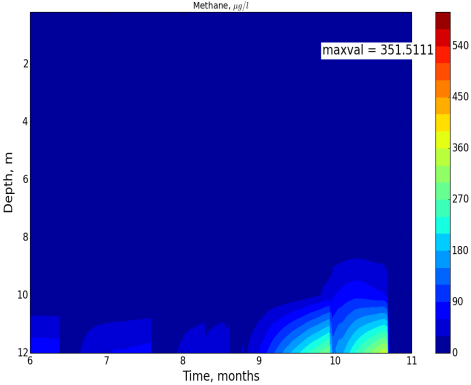

Increased minimal diffusion coefficient ($10 * \lambda_{w0}$)

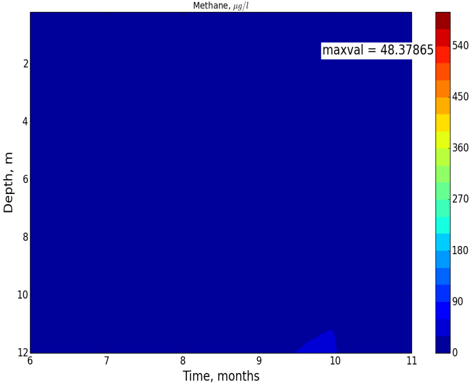

Oxygen diffuses downwards, oxidizing methane

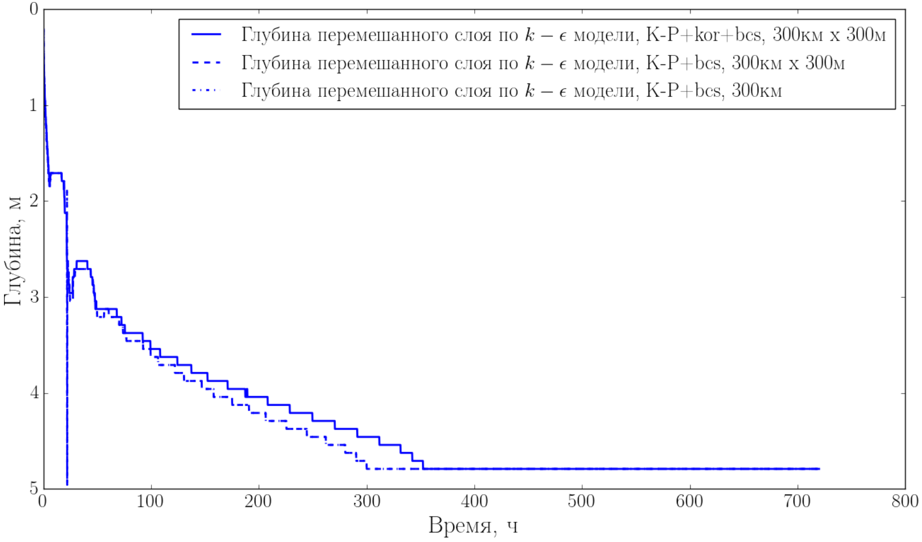

Figure: Эволюция глубины перемешанного слоя в эксперименте К.-Ф., дополненном учетом силы Кориолиса и параметризацией бароклинных сейш (результаты моделирования), при горизонтальных размерах озера: 300 км×300 м и 300 км×300 км

Observations

- Conducted since 2009 by University of Helsinki
- Ultrasonic anemometer USA-1, Metek GmbH
- Enclosed-path infrared gas analyzers, LI-7200, LI-COR Inc.
- Four-way net radiometer (CNR-1)
- relative humidity at the height of 1.5 m (MP102H-530300, Rotronic AG)
- thermistor string of 16 Pt100 resistance thermometers (depths 0.2, 0.5, 1.0, 1.5, 2.0, 2.5, 3.0, 3.5, 4.0, 4.5, 5.0, 6.0, 7.0, 8.0, 10.0 and 12.0 m)
- Turbulent fluxes were calculated from 10 Hz raw data by EddyUH software

Measurement raft

Footprint of the raft measurements

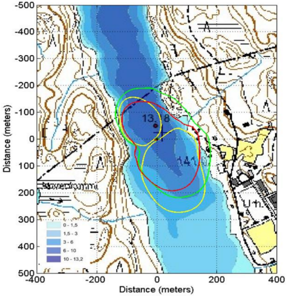

Internal seiche mixing parameterization in $k - \epsilon$ model

Goudsmit et al. 2002

- Shear production is generalized to include seiches $P = \nu_t M^2 + \boxed{P_s}$;
- TKE production by seiche-induced shear at lake's margins
  $P_s = -\frac{1 - C_{diss}\sqrt{C_{d,bot}}}{\rho_{w0} c A_b} \gamma \frac{1}{A} \frac{dA}{dz} N^2 E_s^{3/2}$, E_s - seiche energy;
- Seiche energy is derived from wind forcing: $\frac{dE_s}{dt} = \alpha A_0 \rho_a C_d (u^2 + v^2)^{3/2} - \gamma E_s^{3/2}$
- Stationary Richardson number (Burchard, 2002) may be derived for this case as $Ri_{st} = \frac{Pr \Delta c_{\epsilon 21}}{\Delta c_{\epsilon 23} - \nu_0^{-1} Pr C_s \Delta c_{\epsilon 21} (u^2 + v^2)^{3/2}} \approx 0.30$ for typical wind speed

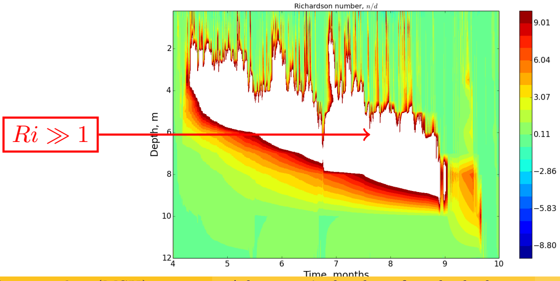

Kato-Phillips experiment

- no heat and radiation flux at the top and bottom boundaries
- constant surface wind stress 0.01 N/m^2
- linear stable initial temperature profile, 2 K/m
- no morphometry
- no rotation
- depth 7 m, 60 vertical computational layers
- 10 days of the model integration

Kato-Phillips experiment results: Standard k-ϵ model

Time-depth distribution of velocity

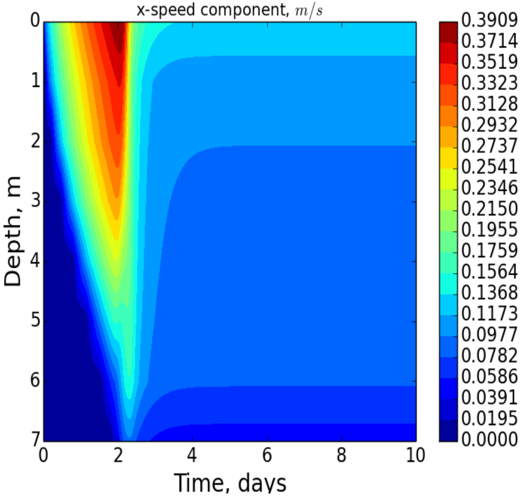

Temperature and eddy conductivity profiles

9-th day

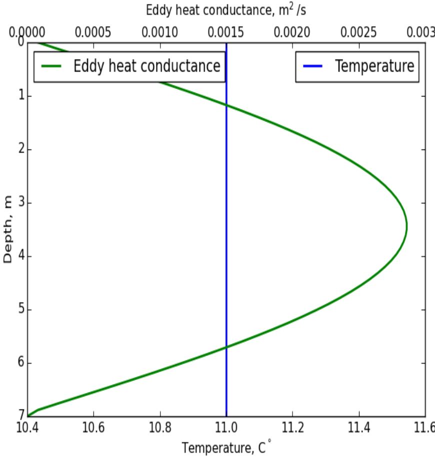

he deepening of the mixed layer follows well the know formula $H_{ML} = 1.05 u_{*w} N_0^{-1/2} t^{1/2}$ (Price, 1979)

After complete mixing of temperature the flow is classical Cuette flow

Kato-Phillips experiment: k-ϵ model + barotropic seiches

Time-depth distribution of velocity

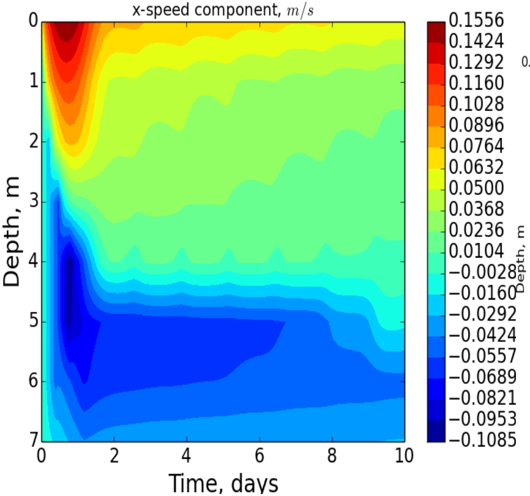

Temperature and eddy conductivity profiles, 9-th day

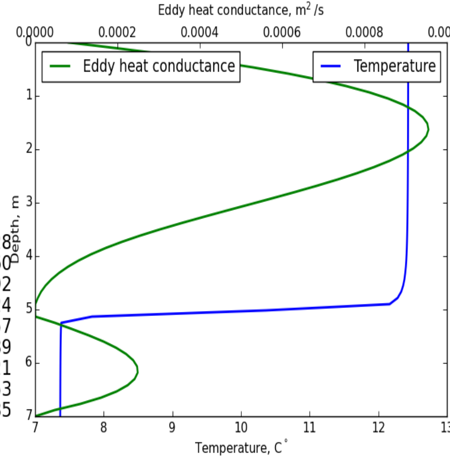

The bottom return flow creates another mixing layer, having very thin extremely stratified interface with the upper one

Kato-Phillips experiment: k-ϵ model + baroclinic seiches

Time-depth distribution of velocity

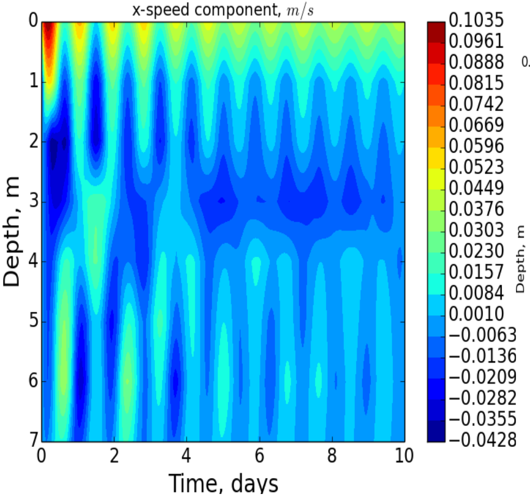

Temperature and eddy conductivity profiles, 9-th day

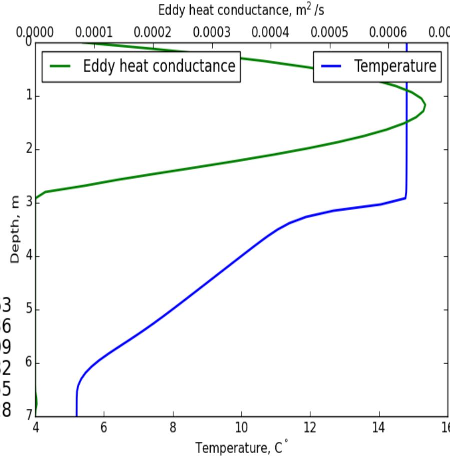

The response of velocity to wind stress is waves, with dominating 1-st vertical mode, ~ 1 day period. The thermocline is preserved, with both surface and bottom mixed layer present

Mixed-layer depth

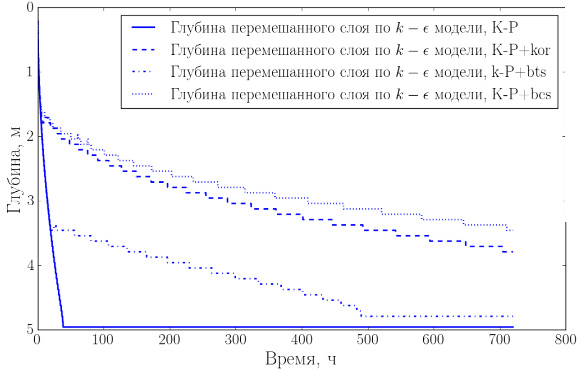

K-P – Kato-Phillips experiment,
K-P+kor – Kato-Phillips experiment with Coriolis force,
K-P+bts – Kato-Phillips experiment with barotropic seiches,
K-P+bts – Kato-Phillips experiment with baroclinic seiches

- Rotation and seiching impose similar suppressing effect on vertical mixing
- Barotropic seiche parameterization is not enough to produce "correct" mixing

Mixed-layer depth

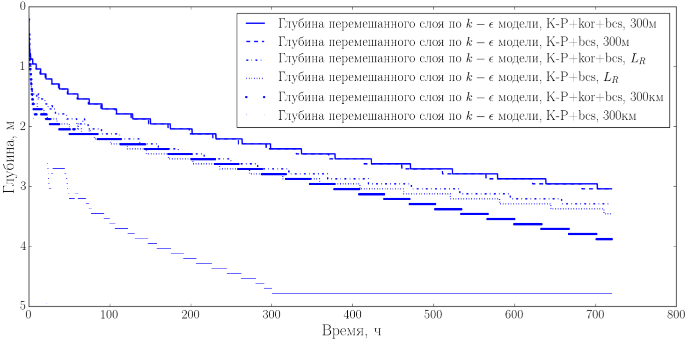

Kato-Phillips experiment with Coriolis force and baroclinic seiches at different lake sizes:
300 m×300 m, $L_R \times L_R$ and 300 km×300 km ($L_R \approx$2.77 km)

- Coriolis force playes significant role in mixing compared to seiching only for the lake size $L \gg L_R$
- The effect of Coriolis force for very large lakes is similar in magnitude to that of seiching for small lakes

Why the mixing is suppressed by rotation and seiching?

- In classical Kato-Phillips setup, the friction is zero at the base of mixed layer, leading to continuous increase of total momentum in mixed layer (under constant momentum flux from the atmosphere), the shear production of TKE and mixed-layer deepening until complete mixing of temperature and achieving stationary Cuette flow (where the momentum flux at the top is compensated by friction at the bottom)
- In both cases of rotation and seiching quasi-stationary oscillatory velocity patterns are established where Coriolis and pressure gradient terms (respectively) "consume" the constant momentum flux from the atmosphere

Пограничные слои в водоемах (данные наблюдений)

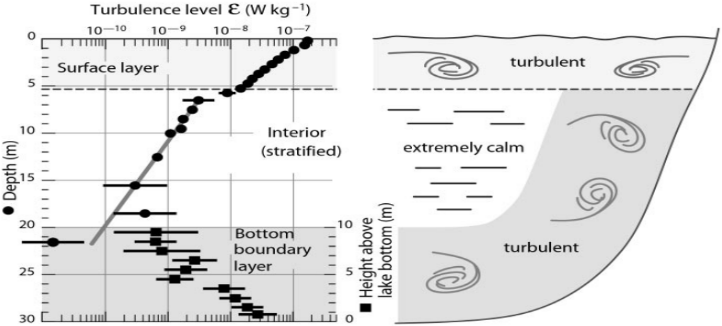

- верхний перемешанный слой – эпилимнион: TKE генерируется в основном за счет сдвига скорости ($\sim$ напряжение трения)
- средний слой – металимнион (термоклин): очень устойчиво стратифицированный
- нижий слой – гиполимнион: генерация TKE за счет сдвига внутренних циркуляций (сейши, волн Кельвина)

Wüest and Lorke 2003, Annu.Rev.Fluid Mech.

Критерий справедливости одномерного приближения

Показано на примере оз.Куйваярви (Финляндия)

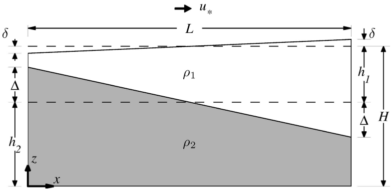

Shintani et al., 2010

Wedderburn number

$$W = \frac{g\Delta\rho h_1^2}{\rho_0 u_*^2 L}$$

$$W_{cr} = \frac{1}{2}$$

Running means

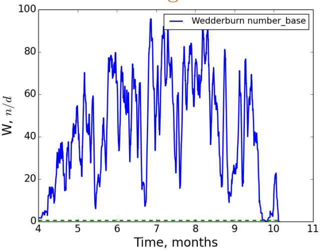

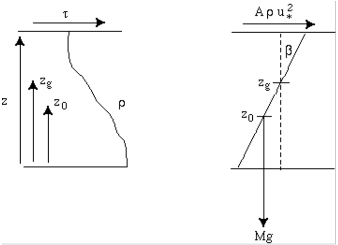

Imerito, 2015

Lake number

$$L_N = \frac{2(z_m - z_v)V\rho_0 g h_1}{z_v \tau A_0 L}$$

$$L_{N,cr} = 1$$

Thermocline displacement is negligible compared to mixed-layer depth

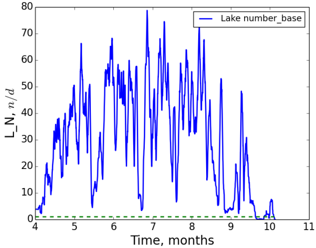

Схемы маршрутизации водотоков (на примере TRIP)

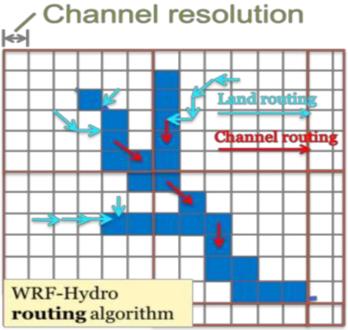

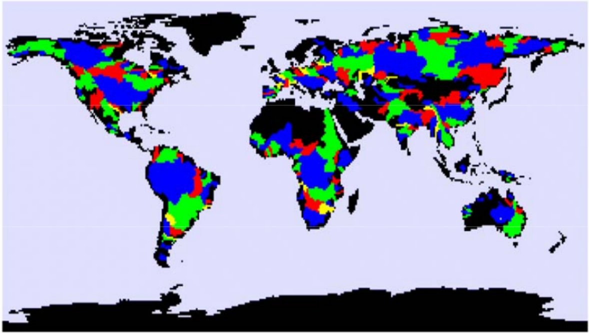

- Вычислительно простые схемы, достаточные для воспроизведения средних расходов
- Диагностические формулы для расхода рек -> не воспроизводят экстремальные явления
- Нет расчета термодинамики и льдообразования
- Не учитываются биогеохимические процессы

Модели водоема в климатических моделях и системах прогноза погоды

Модель климата/прогноза погоды	Модель водоема
IFS (ECMWF)	FLake
UKMO (MetOffice)	FLake
COSMO (European Consortium)	FLake
HIRLAM (European Consortium)	FLake
CESM (US consortium)	CLM-LISSS4
CRCM (Canada)	Flake/Hostetler
WRF (Penn SU)	FLake
...	...

Модель пузырька

For shallow lakes (several meters), bubbles reach water surface not affected, for deeper lakes bubble dissolution has to be taken into account.

- Five gases are considered in a bubble: $CH_4,\ CO_2,\ O_2,\ N_2,\ Ar$
- Bubbles are composed of CH_4 and N_2 when they are emitted from sediments
- The velocity of bubble, v_b, is determined by balance between buoyancy and friction
- The molar quantity of i-th gas in a bubble, M_i, changes according to gas exchange equation (McGinnis et al.,

$$\frac{dM_i}{dt} = v_b \frac{\partial M_i}{\partial z} = -4\pi r_b^2 K_i (H_i(T) P_i - C_i).$$

- Gas exchange with solution is included in conservation equation for i-th gas :

$$\frac{\partial C_i}{\partial t} = \frac{1}{A}\frac{\partial}{\partial z} Ak \frac{\partial C_i}{\partial z} + \boxed{\frac{1}{A}\frac{\partial AB_{C_i}}{\partial z}} +$$

$$F(z,t,C_i,A) + (H_{C_i} - \boxed{B_{C_i,b}})\frac{1}{A}\frac{dA}{dz}.$$

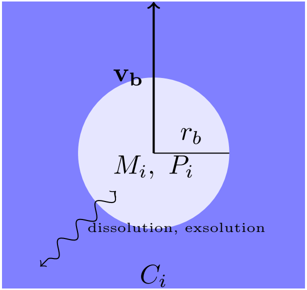

Methane ebullition
from different soil columns